Astron. Astrophys. 138, 10–18 (1984)

ASTRONOMY AND ASTROPHYSICS

IRAS* measurements of planetary nebulae

S. R. Pottasch[1], B. Baud[2], D. Beintema[2], J. Emerson[3], H. J. Habing[4], S. Harris[3], J. Houck[5], R. Jennings[6], and P. Marsden[7]

[1] Kapteyn Astronomical Institute, Groningen, The Netherlands
[2] Space Research Laboratory, Groningen, The Netherlands
[3] Queen Mary College, London, England
[4] Sterrewacht Leiden, Leiden, The Netherlands
[5] Department of Astronomy, Cornell University, Ithaca, NY, USA
[6] University College, London, England
[7] University of Leeds, England

Received March 1, accepted April 10, 1984

Summary. Far-infrared IRAS measurements of 46 of the brighter planetary nebulae are presented. Dust temperatures are computed. Higher dust temperatures are found in the younger, denser nebulae. Lyman α is shown to be a sufficient source of energy to heat the dust for the larger, older nebulae, but another energy source (probably the exciting star) is required for the younger nebulae.

Key words: dust – planetary nebulae – far infrared radiation

I. Introduction

With the measurement of 10 μm emission from NGC 7027 in 1967 by Gillett et al., it became clear that a strong excess of continuous radiation may be emitted from planetary nebulae in the infrared. In the intervening years the characteristics of the radiation have been studied for that part of the infrared accessible from the ground by different authors (e.g., Cohen and Barlow, 1974, 1980). Several studies have been made, the most extensive of which is the measurement of 12 nebulae in several wavelength bands from an aircraft (Moseley, 1980). Since the launch of the IRAS satellite in January 1983 measurements have been made of at least 500 known planetary nebulae and a yet undetermined number of objects which may be identified with planetaries in the future.

It is the purpose of this paper to report on a selection of 46 nebulae that were chosen for a variety of reasons. First, 10 nebulae observed by Moseley are discussed in order to compare the IRAS measurements with earlier measurements. Second, the stronger sources were selected, preferably those observed in all four bands, but at least seen at 25 μm, 60 μm, and 100 μm. Third, nebulae well studied in other wavelength regions were selected. Fourth, both low surface brightness and high surface brightness nebulae were chosen.

The far-infrared radiation makes it possible to study the bolometric flux of the emitting dust. The part of the spectrum available from the ground is too limited because the peak of the infrared flux usually lies between 25 μm and 100 μm. It is not the purpose here to go deeply into the dust properties. The measurements will be presented in Sect. II and compared with existing measurements in Sect. III. A discussion of the "temperature" of the dust, principally based on the observed spectral distribution in the far infrared, will be given in Sect. IV. The energy source for the dust heating will be discussed in Sect. V.

Send offprint requests to: S. R. Pottasch, Kapteyn Laboratorium, Zernike Gebouw, Postbus 800, 9700 AV Groningen, The Netherlands

* The Infrared Astronomical Satellite was developed and is operated by the Netherlands Agency for Aerospace Programs (NIVR), the U.S. National Aeronautics and Space Administration (NASA) and the U.K. Science and Engeneering Research Council (SERC)

II. IRAS observations

A description of the IRAS survey instrument has already been given (Neugebauer et al., 1984). In surveying the sky, the same position was measured at different times, with intervals spaced at seconds, hours, weeks and sometimes months. In all cases reported here, at least three "seconds confirmed" measurements (two measurements spaced seconds apart) were made. Usually four to six "seconds confirmed" measurements were available at all bands. "Seconds confirmed" measurements always reappeared at least once on subsequent orbits to form an "hours confirmed" pair. In the large majority of cases two "hours confirmed" measurements were available and in 14 cases three "hours confirmed" measurements have been made. This is true as well for each of the individual wavelengths bands where a positive detection is reported, although occasionally an individual detector showed no response. The individual flux measurements at a given wavelength for single objects are usually within 15% of each other, although departures as large as 30% occasionally occur.

About one third of the nebulae (14) have been remeasured after a six month interval. The reproducibility of the measurements is excellent. Fluxes deduced independently from the second set of measurements almost always agree within 30%. Since the scan direction usually differs by about 180° in two periods, this also argues against confusion.

Finally, the nebulae have been identified on (spline fitted) maps of the sky made from the survey measurements at 60 μm and 100 μm. The nebulae stand out clearly on the 60 μm maps and no case of a nearby confusing source has been found. At 100 μm there is also no evidence for confusion.

Table 1 lists the results. The first column gives the NGC number and the second column gives the Perek-Kohoutek designation. The third and fourth columns list the observed IRAS position of the nebula. These are almost always within 10″ of the optical position. This accuracy is somewhat better than given in the above reference and is probably due to the fact that the sources are quite strong and in regions generally free of confusion. The

Table 1. IRAS measurements of planetary nebulae

	Observed Coordinates (1950)			Observed Flux Density (Jy)			
NGC	PK	RA	DEC	12 μm	25 μm	60 μm	100 μm
246	118-74.1	0 44 30.9	-12 08 44	0.77	23.5	38.	34.
1501	144+ 6.1	4 02 41.3	60 47 10	1.1	6.0	17.	14.
I 418	215-24.1	5 25 10.0	-12 44 17	35.	224.	129.	42.
2346	215+3.1	7 06 50.0	- 0 43 35	0.45	0.9	8.6	17.
2371/2	189+19.1	7 22 25.9	29 35 25	0.6	6.1	9.2	11.
2392	197+17.1	7 26 13.2	21 00 56	0.75	10.	22.	19.
2438	231+ 4.2	7 39 32.8	-14 36 59	< 0.2	1.1	7.4	13.
2440	234+ 2.1	7 39 42.1	-18 05 26	3.4	29.	50.	32.
A 30	208+33.1	8 44 03.4	18 03 46	2.0	45.	104.	61.
2818	261+ 8.1	9 13 59.9	-36 24 59	< 0.2	1.0	2.5	3.4
2867	278- 5.1	9 20 00.4	-58 05 49	2.0	16.	19.	10.
2899	277- 3.1	9 25 31.0	-55 53 17	0.3	1.6	5.9	14.
3195	296-20.1	10 09 57.1	-80 36 39	< 0.14	1.0	7.2	7.8
3242	261+32.1	10 22 21.3	-18 23 17	4.4	38.	63.	36.
4361	294+43.1	12 21 54.3	-18 30 23	0.5	9.4	10.	8.3
He 2-131	315-13.1	15 32 00.0	-71 45 17	6.2	110.	74.	29.
6072	342+10.1	16 09 42.3	-36 06 12	0.4	3.3	28.	42.
Cn 1-1	330+ 4.1	15 47 37.9	-48 35 59	18.	43.	20.	14.
Mz 3	331- 1.1	16 13 23.4	-51 51 47	78.	352.	322.	144.
6153	341+ 5.1	16 28 05.5	-40 08 49	6.5	54.	140.	68.
6210	43+37.1	16 42 23.8	23 53 26	2.0	27.	40.	21.
6302	349+ 1.1	17 10 21.3	-37 02 43	31.	363.	1000.	840.
6543	96+29.1	17 58 34.3	66 37 56	7.8	118.	158.	80.
6572	34+11.1	18 09 40.6	6 50 26	23.	177.	117.	40.
6751	29- 5.1	19 03 15.3	-6 04 10	4.1	19.	28.	10.
A 58	37- 5.1	19 15 48.7	1 41 27	4.9	31.	47.	21.
6781	41- 2.1	19 16 01.5	6 26 47	0.6	2.6	49.	93.
Vy 2-2	45- 2.1	19 21 59.1	9 47 57	15.	100.	49.	13.
BD+30 3639	64+ 5.1	19 32 47.3	30 24 17	78.	240.	200.	89.
6818	25+17.1	19 41 07.8	-14 16 28	1.4	18.	22.	15.
6826	83+12.1	19 43 27.2	50 24 05	5.1	41.	54.	28.
6884	82+ 7.1	20 08 48.1	46 18 34	1.1	15.	21.	6.?
6881	74+ 2.1	20 09 01.9	37 15 44	2.7	20.	22.	< 17.
6886	60- 7.2	20 10 29.4	19 50 17	1.1	12.	14.	7.8
6891	54-12.1	20 12 47.1	12 33 01	0.9	11.	16.	8.4
I 4997	58-10.1	20 17 51.4	16 34 20	2.3	28.	12.	3.8
6905	61- 9.1	20 20 09.1	19 56 37	0.5	6.7	10.	8.7
7008	93+ 5.2	20 59 04.7	54 20 50	1.5	27.	57.	49.
7009	37-34.1	21 01 27.6	-11 33 47	6.2	49.	111.	56.
7026	89+ 0.1	21 04 36.0	47 39 00	2.3	21.	49.	39.
I 5117	89- 5.1	21 30 37.2	44 22 30	11.	50.	28.	10.
Hu 1-2	86- 8.1	21 31 07.9	39 24 43	0.5	4.2	4.9	2.3
K 4-45	96+ 1.1	21 33 40.8	53 33 42	6.7	41.	223.	358.
7094	66-28.1	21 34 27.2	12 33 50	< 0.2	1.2	4.2	3.8
7662	106-17.1	23 23 29.9	42 15 38	3.7	37.	43.	20.

eventual IRAS position should be accurate to within 10″ to 20″. The last four columns give the preliminary measured flux density in Jy (10^{-26} W m^{-2} Hz^{-1}) at the stated wavelengths assuming blackbody emission at the temperature deduced from the "in band" flux ratios. The statistical uncertainties are typically 15%. The calibration is preliminary, but is probably within 30% of its ultimate value at 60 and 100 μm, and possibly better at 12 and 25 μm. All of the nebulae are smaller than the effective size of the detector so that the measurements always refer to the total flux. Even if the infrared emission comes from an area considerably larger than the ionized nebula, the total infrared flux would still be contained within the beam of a single detector.

III. Comparison with previous measurements

In Fig. 1 the IRAS measurements are plotted for the 10 nebulae observed in common with Moseley (1980). The latter measurements are also plotted (the points at 37 μm, 52 μm, 70 μm, and 108 μm) together with some other measurements above 8 μm (Gillett and Stein, 1970; Gillett et al., 1971; Cohen and Barlow, 1974). The agreement is quite satisfactory for BD+30 3693, NGC 6572, IC 4997, and NGC 6543, but less good for the other nebulae. For IC 418 Moseley measured peaks at two wavelengths in the spectrum. This is no longer seen in the IRAS measurements, indicating that the continuous energy distribution is very similar

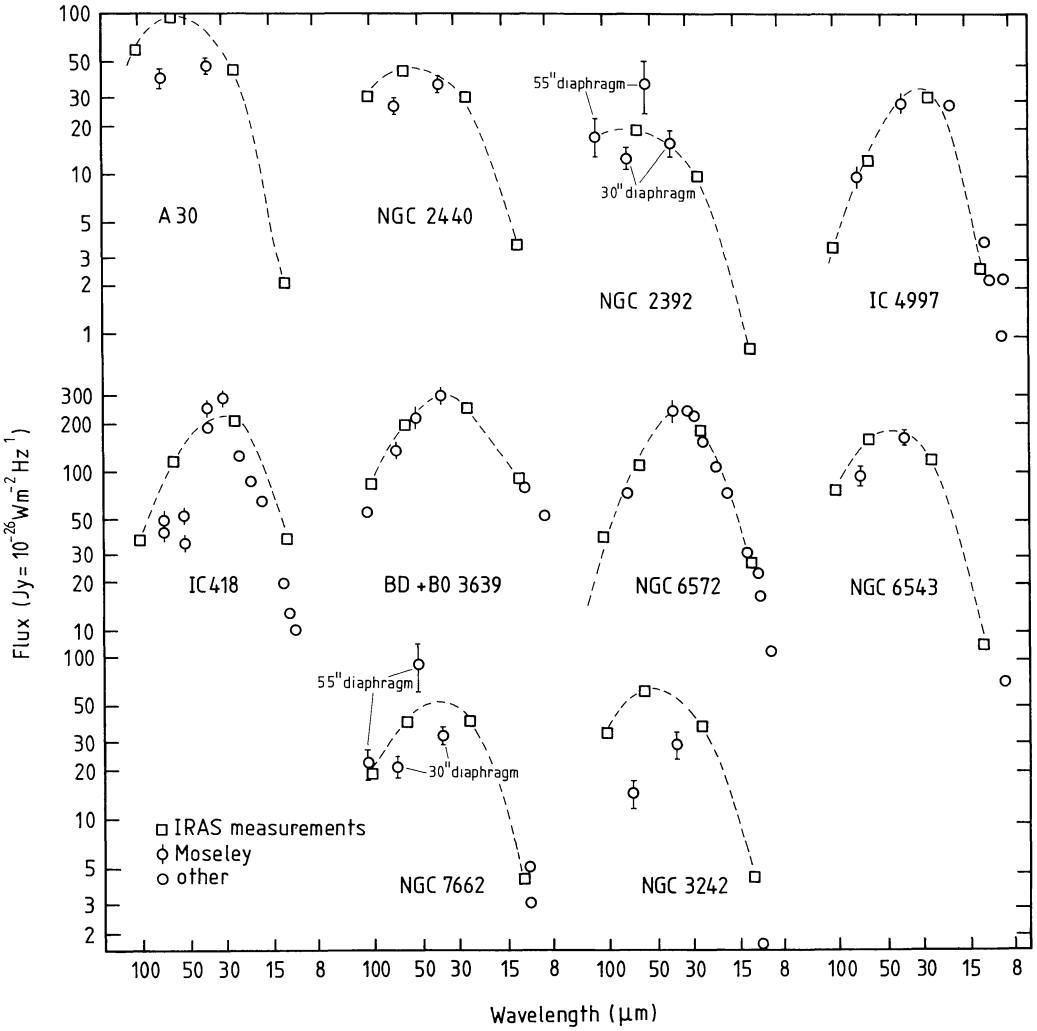

Fig. 1. The measured infrared flux densities are plotted as a function of wavelength for those nebulae which have been measured from an aircraft. The IRAS measurements are shown as open squares. The measurements of Moseley (1980) are shown as open circles with an error bar. The other circles are taken from other observers

to other nebulae. Furthermore, the IRAS measurements indicate substantially more emission for the nebulae NGC 3242 and A 30 than reported by Moseley and a shift of the peak emission toward longer wavelengths. Moseley also reported observing substantially more emission from the nebulae NGC 7662 and NGC 2392 when observing with a 55″ diameter diaphragm. The IRAS measurements fall in between Moseley's measurements, throwing some doubt as to the reality of this difference.

A general difference between the measurements given by Moseley and the IRAS measurements is the following. It would appear from Moseley's measurements that the peak emission occurs close to 30 μm. The IRAS measurements of the same 10 objects indicate that there is a wider range of wavelengths for which the peak value of emission F_ν occurs. This is between 30 μm and 60 μm. Studying the sample of 46 nebulae given in Table 1 leads to the conclusion that the peak wavelength has a still wider range, from 20 μm to above 100 μm. There are 11 objects, almost one quarter of the sample, where the highest value of F_ν occurs at, or possibly beyond, 100 μm.

Recently, Shure et al. (1983) have measured the spectrum near 25 μm of eight of the nebulae included in Table 1. There is satisfactory agreement between their continuum fluxes measured at 25.87 μm and the IRAS 25 μm band fluxes for seven of the objects (satisfactory agreement is defined as when the 2σ error of Shure et al., and the 20% IRAS uncertainty overlap). For one object, NGC 7662, the IRAS flux is more than a factor of two greater than the continuum measurement of Shure et al. Part of this difference is the inclusion of the strong O IV line at 25.87 μm in the IRAS flux. The strength of this line as reported by Shure et al. would account for 25% of the IRAS flux. It is not expected that there will be other lines in this IRAS band strong enough to account for the remaining missing flux. The difference is more likely to be sought in faint radiation outside of the 30″ diaphragm used by Shure et al.

There seems to be a systematic difference of 10 to 15% between the continuum measurements of Shure et al. and the larger IRAS 25 μm flux. It is possible that line emission contributes to this difference, though it is not in general expected that this will be a major contributor for most of the nebulae in the 25 μm band.

Line emission will be relatively more important in the 12 μm band since continuum radiation is often considerably smaller in this band and several potentially strong lines occur in it. A more

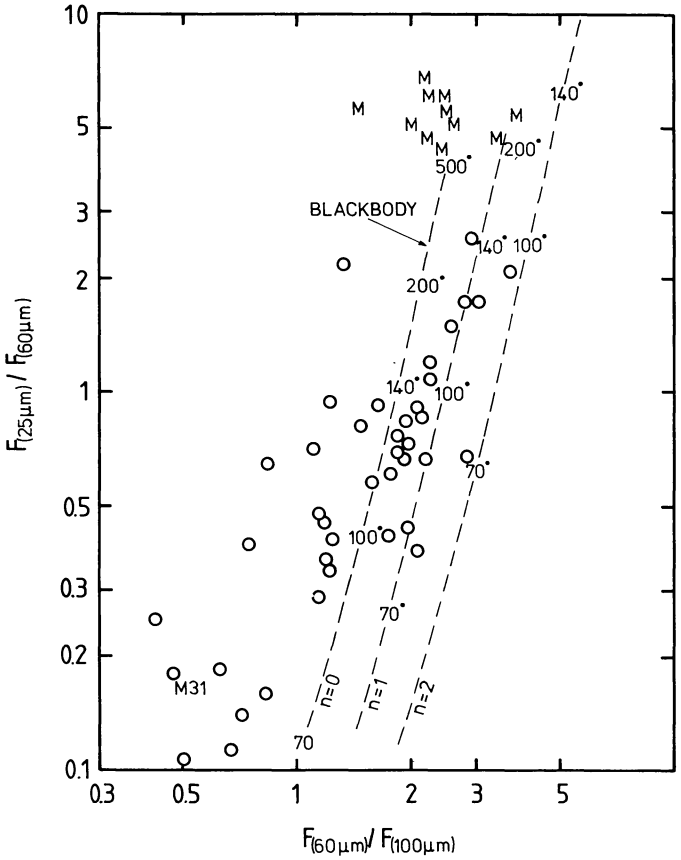

Fig. 2. A colour-colour plot for those planetary nebulae observed at 25 μm, 60 μm, and 100 μm. A blackbody line is also shown as well as the position of a blackbody multiplied by an emissitivity proportional to λ^{-n}. The temperatures are marked on the theoretical curves. The point marked M31 refers to measurements of the central bulge of the Andromeda nebula. The points labled *M* are Mira stars, shown for comparison

detailed discussion is given elsewhere (Pottasch et al., 1984), where it is shown that in some of the nebulae investigated the lines can contribute half of the observed flux in this band.

IV. Temperature of the emitting dust

The ratio of the flux observed in the different wavelength bands is a measure of the color temperature of the emission. Figures 2 and 3 are color-color diagrams which plot the ratio of the fluxes in different wavelength bands against each other. In Fig. 2 the ratio $F(25\,\mu m)/F(60\,\mu m)$ is plotted as ordinate against the ratio of $F(60\,\mu m)/F(100\,\mu m)$. While the points show a considerable amount of scatter (the scatter is real), there is a clear correlation between the two ratios. A correlation is to be expected as a result of changing one or more of the physical parameters in the emitting dust. For example, suppose the dust radiated as a blackbody of temperature T_D and that this temperature was constant for the dust in a given nebula. Then the expected correlation would be that given by the dashed line in the figure, where the positions for three different values of T_D are marked. This model gives a fair representation of the points but it is clear that the observed slope is different from the predicted slope. Another model often mentioned (see the review of Barlow, 1983) is the same constant temperature dust but now with an emissivity proportional to λ^{-n} where n is often taken to be either 1 or 2. The results of this model are shown as the dot-dashed line in the figure, again with different values of T_D marked. This latter model clearly gives a worse fit to the observations than the former, since not only does it have the same incorrect slope but it is also displaced away from the locus of the observed points.

The models used above refer to dust of a constant temperature. If a temperature gradient was present in the dust it would shift the bottom parts of the curves further toward the left of the diagram. Thus it may be possible to interpret the observations with a different value of n and a temperature gradient. This discussion will be carried further in Sect. VII and in a future paper.

Figure 3 shows the color ratios involving the 12 μm, 25 μm, and 60 μm fluxes. The scatter is greater in this diagram. The correlations expected from the two models previously described are also given. As discussed above the 12 μm flux is only partly continuum radiation. Often more than 50% of it is due to radiation from atomic lines, principally SIV (10.56 μm), NeII (12.8 μm), and NeIII (15.5 μm). This is probably what causes the large amount of scatter in Fig. 3 and makes any use of 12 μm flux subject to the greatest caution. The other bands are less affected by line radiation, although the contribution of the OIV (25.87 μm) line to the 25 μm flux will sometimes be substantial.

For the next sections of this paper a model of constant T_D dust emitting as a blackbody with constant emissivity will be used. The value of T_D is determined by the best fit to the observed points in a given nebula, where the 12 μm point is not used (except as an upper limit). A good representation to the observed points can be determined in this way. Whether this is the correct model or not, the value of T_D (given as the second column of Table 2) is a useful parameter for representing the observed spectral distribution in the far infrared.

In the third and fourth columns of Table 2 the distance d and the radius R of each nebula is given. This is computed from the angular size of the nebula and its distance. The distance is taken from a compilation of Pottasch (1983). The values of R are plotted against T_D in Fig. 4. A fairly clear correlation between these two quantities can be seen. The smaller and presumably younger objects have the hotter dust. If the emitting dust is mixed with the ionized matter or at least is very close to it [which appears to be the case in NGC 7027 from the far infrared maps of Bentley (1982) and Aitken and Roche (1983)] then the hotter dust would be expected in the smaller nebulae. This is because the radiation field is less dilute in these nebulae. In addition, the smaller nebulae are younger and have a lower temperature exciting star and thus a relatively stronger radiation field longward of $\lambda = 912$ Å, where the gas is not competing so strongly to absorb photons. As will be seen in the next section, this optical radiation produces an important contribution to the energy balance of the dust.

V. On the energy source for the dust heating

It has been shown in the previous section that the temperature of the dust is correlated with the radius of the nebula. This correlation with nebular properties implies that the source of energy for heating the dust is the nebula and its central star. It was

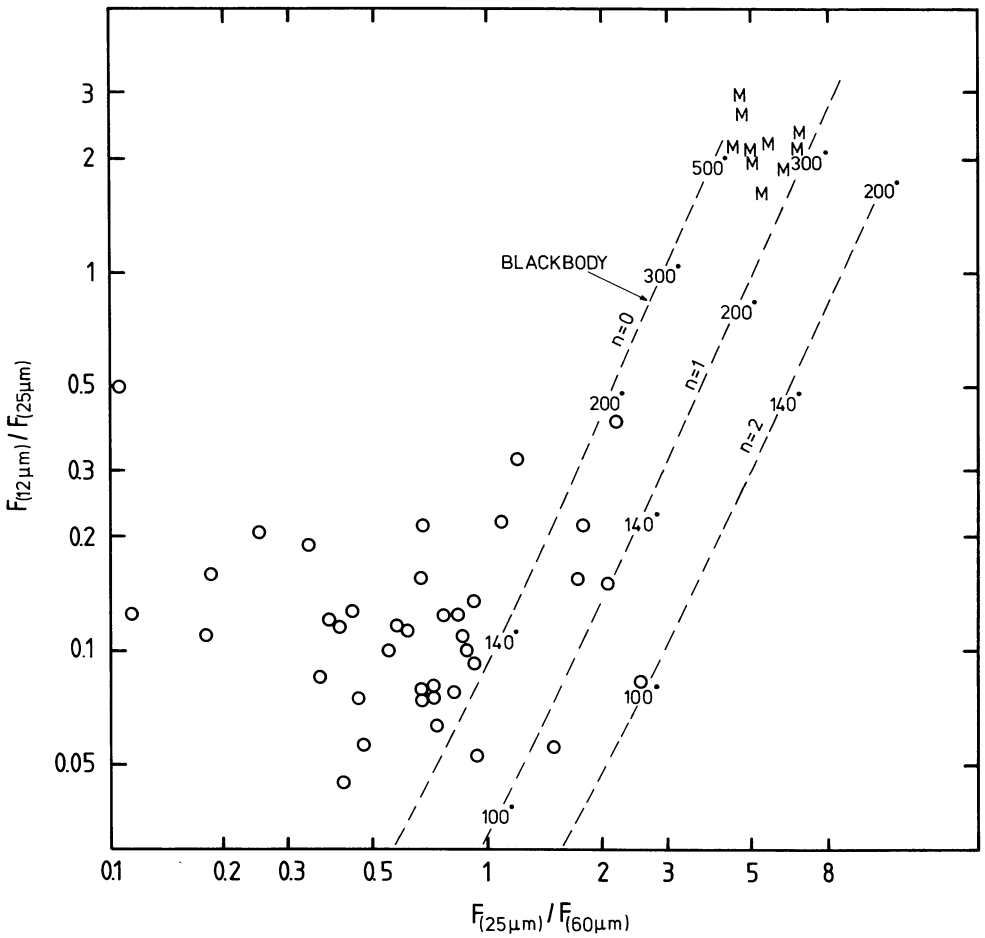

Fig. 3. Same as Fig. 2 for different wavelengths including 12 μm. The 12 μm band contains nebular line emission as well as dust continuum so that the 12 μm fluxes are only an upper limit to dust emission

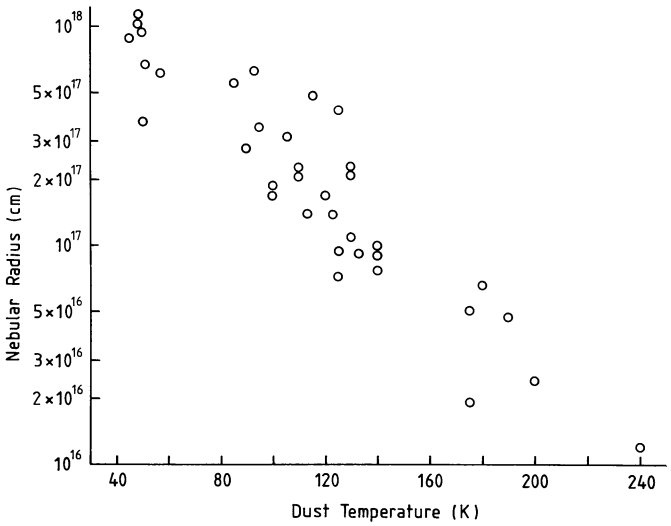

Fig. 4. The dust temperature as defined by the best fitting blackbody curve through the 25 μm, 60 μm, and 100 μm fluxes is plotted against the radius of the nebula

suggested by Krishna Swamy and O'Dell (1968) that at least an important part of the energy is transmitted to the dust by the Lyman α radiation generated in the nebula. This is quite plausible since the optical depth for Lyman α radiation in the nebula is expected to be high with the consequence that the mean free path for a Lyman α photon will be many times the geometrical size of the nebula.

The total amount of energy observed in the infrared (F^{IR}_{total}) from the nebulae presented above is listed in Column 5 of Table 2. It is simply the energy under the curve defined by the points listed for each nebula in Table 1. If necessary an extrapolation was made to shorter or longer wavelengths than measured by IRAS, but in no case did this extrapolation affect the value of F^{IR}_{total} in an important way. The values of F^{IR}_{total} have been plotted against the observed nebular 6-cm radio continuum flux density in Fig. 5. (For convenience the observed 6-cm radio continuum flux density is listed in Column 7 of Table 2. They are taken mainly from Milne and Aller (1975, 1983) and from Higgs (1971). It is clear from the figure that a strong correlation exists between F^{IR}_{total} and the radio flux.

What contribution does Lyman α make to the infrared radiation? If all the Lyman α produced by recombination in the nebula heats the dust the amount of far infrared emission will be:

$$F^{IR}_{total} = 3.98\,10^{-14} S_\nu T_e^{-0.53} \nu^{-0.1} Y^{-1} \cdot \frac{I(\mathrm{Ly}\alpha)}{I(\mathrm{H}\beta)}\,\mathrm{W\,m^{-2}}, \quad (1)$$

where S_ν is the radio continuum emission in mJy, T_e the electron temperature, ν is the frequency of the radio measurement in GHz, Y depends on the helium content and $I(\mathrm{Ly}\alpha)/I(\mathrm{H}\beta)$ is the theoretical intensity of these two lines.

Table 2. Dust temperatures and total infrared fluxes

NEBULA NGC, etc.	T_D	d	R	F^{IR}_{total}	$L^{IR}/L_\odot$	S_ν (5 GHz)	Infrared excess	$M_D/M_\odot$	M_D/M_G
	°K	Kpc	10^{17} cm	10^{-12} W m^{-2}		mJy	IRE		
246	60	0.5	8.9	4.5	35.	247.	2.8	23. $\times10^{-5}$	7.6 $\times10^{-4}$
1501	85	1.4	5.7	1.3	76.	210.	0.98	17. "	
IC 418	190	0.42	0.47	39.	210.	1550.	2.7	1.9 "	24. "
2346	50	0.9	3.7	0.7	17.	86.:	1.3:	32. "	43. "
2371/2	90	0.7	2.8	1.2	18.	87.	2.2	3.2 "	2.4 "
2392	95			2.5		251.	1.5	-	-
2438	48	2.0	10.2	0.58	70.	83.	1.1	153. "	-
2440	115	2.0	4.9	5.3	630.	410	2.0	43. "	5.9 "
A30	105			9.2				-	-
2818	51	1.8	6.8	0.21	20.	33.	1.0	35. "	3.0 "
2867	130	2.0	2.3	3.0	360.	252.	1.9	15. "	10. "
2899	40			0.54		84.	1.0	-	-
3195	67			0.51		33.	2.4	-	-
3242	115	0.75	2.3	7.5	130.	860.	1.4	8.5 "	8.2 "
4361	125	0.9	4.2	1.6	39.	205.	1.2	1.9 "	1.8 "
He2-131	175	1.0	0.5	22.	660.	325.	7.2	8.2 "	78. "
6072	50	1.8	9.5	1.9	185.	152.	1.9	345. "	-
Cnl-1	215			8.5		38.	24.	-	-
Mz-3	160			58.		630.	15.	-	-
6153	106	1.8	3.2	12.1	1170.	477.	3.1	109. "	21. "
6210	130	0.6	0.77	5.4	58.	300.	2.8	2.4 "	15. "
6302	100	0.5	1.7	87.	653.	3488.	3.1	76. "	45. "
6543	125	0.6	0.72	21.	227.	850.	3.1	11. "	120. "
6572	180	0.6	0.66	33.	356.	1307.	2.7	4. "	25. "
6751	130	1.5	2.4	3.8	260.	63.	9.5	11. "	38. "
A 58	122			6.0					-
6781	48	1.5	11.9	3.4	230	350	1.5	42. $\times10^{-5}$	-
Vy2-2	230	1.5		22.		220	10.	6.2 "	-
BD+30 3639	175	0.5	0.19	49.6	372	600	8.8	4.6 "	340. $\times10^{-4}$
6818	123	1.0	1.4	3.3	100	300	1.2	5.0 "	14. "
6826	120	0.9	1.7	4.0	97	385	1.3	5.5 "	9.5 "
6884	140	2.0	0.9	2.7	324	200	1.7	10. "	33. "
6881	150			3.2		180	1.9	-	-
6886	130	2.0	1.1	2.2	264	108	2.7	11. "	14. "
6891	125	1.0	0.95	2.2	66	105	3.0	3.2 "	18. "
IC 4997	185	1.0	0.12	7.8	234	127	6.5	2.3 "	200. "
6905	110	0.6	2.1	1.3	14	52	3.9	1.1 "	2.3 "
7008	95	1.0	6.4	5.8	174	250	3.6	25. "	6.7 "
7009	113	0.7	1.4	13.	191	750	2.5	14. "	13. "
7026	100	2.3	1.9	4.9	780	260	2.9	91. "	29. "
IC 5117	190	2.5	0.24	12.	2250	230	5.6	20. "	320. "
Hul-2	133	1.5	0.92	0.86	58	155	0.87	2.2 "	6.6 "
K4-45	55			13.				-	-
7094	65			0.3		17.	2.7	-	-
7662	140	0.9	1.0	6.8	165	600	1.6	5.0 "	16. "

For $T_e = 10^4$ K, $\nu = 5$ GHz, and $Y = 1.3$, the far infrared emission becomes

$$F^{IR}_{total} = 6.32 + 10^{-15} S_\nu \text{ W m}^{-2} \quad \text{(low density)}, \tag{2}$$

$$= 9.38 + 10^{-15} S_\nu \text{ W m}^{-2} \quad \text{(high density)}. \tag{3}$$

The reason for the difference between the low and high density case is that in the low density gas recombination to the 2*s* level results in twophoton emission which escapes from the nebula while at higher densities collisional excitation from the 2*s* to 2*p* level converts this to Lyman α radiation. The transition between the two cases occurs at a density of about 10^4 cm^{-3}.

Equations (2) and (3) are also shown in Fig. 5 and may be compared to the observations. It seems clear from the figure that the Lyman α radiation is a sufficient source of energy for most of the nebulae whose dust temperature is less than 110 K. The nebulae with higher dust temperatures require, on the average, a factor of 3 more energy than is available from the Lyman α radiation. Therefore some other source of energy beside Lyman α is required.

The infrared excess (IRE) is defined as the ratio of the observed infrared total emission to the energy available in Lyman α photons. Its value is given for the individual nebulae in the 8th column of Table 2. Values of unity indicate that there is sufficient

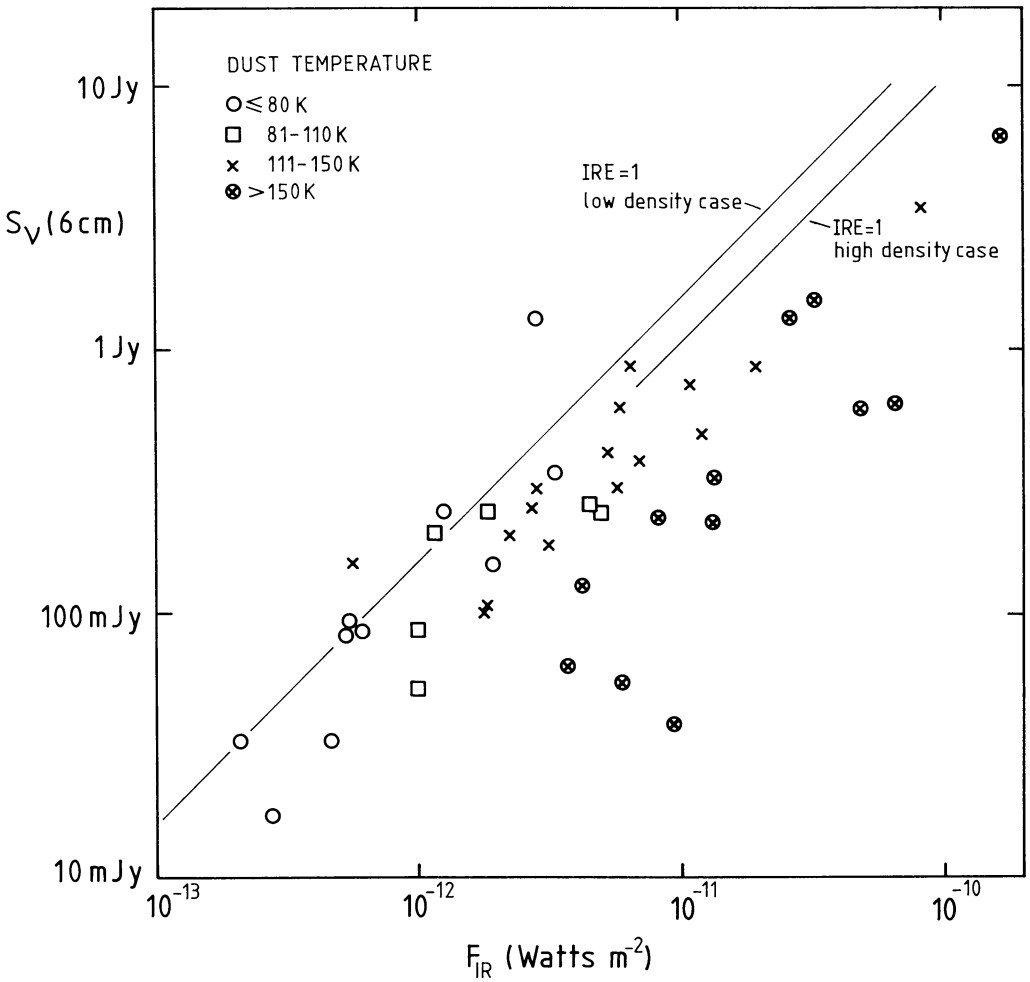

Fig. 5. The total infrared flux for each nebula is plotted against the 6 cm radio continuum flux. The different symbols refer to the various dust temperatures. The line shows the relation expected if the energy source for heating the dust is Lyman α emission produced in the nebula and completely absorbed by the dust

energy in the Lyman α radiation to explain the observed infrared emission. Values somewhat greater than unity, perhaps even as high as two, could be explained by absorption of other nebular line radiation. The most likely candidates are the CIV lines near λ 1550 Å, which like Lyman α, are resonance lines and therefore scattered many times before they leave the nebula.

The very high infrared excesses, however, usually are found in the small, high dust temperature nebulae, which are excited by comparatively bright, low temperature stars. It seems likely that this dust absorbs energy directly from these stars, because this seems to be the only way to explain the rather high values of the IRE. The radiation absorbed by the nebula could be either on the longwave or shortwave side of Lyman α. Because all the cases where the infrared excess is high are young nebulae which contain a large proportion of energy on the longwave side of Lyman α, it is likely that this radiation is more important.

VI. Effect of the absorption of stellar radiation on the temperature determination of the central star

The infrared energy emitted originates in the central star irrespective of whether or not the dust absorbs radiation directly from the star or whether it is first transformed into nebula radiation and then absorbed. It is therefore interesting to compare the total radiation emitted by the central star with that reradiated in the infrared.

This has been done for those nebulae for which a central star temperature has been determined by the energy balance method (Preite-Martinez and Pottasch, 1983). The radius of these stars has been computed using the visual magnitudes and extinctions listed by Pottasch (1984), and assuming the stars radiate as blackbodies. For NGC 7009 the magnitude given by Mendez et al. (preprint, 1984) was used. The resultant stellar luminosities are given in Column 2 of Table 3 (using the same distance as listed in Table 2). It can be seen from this table that in general there is sufficient stellar radiation to explain the observed infrared emission (luminosities given in Column 3 of Table 3 and Column 4 of Table 2). In a few cases a problem arises: in He 2-131, 6572, and IC 4997 it appears that either the temperature or radius of the star has been underestimated.

The same difficulty can arise with the Zanstra temperature. In those cases in which a substantial fraction of the ionizing stellar photons is absorbed by the dust, the temperature determined from the method will be too low. This appears to be unimportant in the large majority of the nebulae, but should be taken into consideration in the small nebulae, including BD+30 3639 and possibly 6210. For these nebulae the Zanstra temperature must be regarded with caution. A more realistic temperature may be computed with the help of measured infrared flux.

Table 3

Nebula	$L_{star}/L_\odot$	$L_{IR}/L_\odot$
246	1080	35
IC 418	560	210
2371	66	18
2438	400	70
2867	2860	360
3242	510	130
He 2−131	420	660
6210	85	58
6572	320	356
6751	1070	260
6781	875	230
BD +30 3639	525	372
6818	650	100
6826	780	97
6853	70	4
6886	1200	264
6891	360	66
IC 4997	265	234
6905	38	14
7009	416	191
7026	1340	780
7662	1230	165

VII. The emissivity as a function of wavelength

As discussed in Sect. IV and can be seen in the color-color diagrams, Figs. 2 and 3, the observations do not clearly show how the emissivity Q varies with wavelength in the far infrared. A reasonable fit to the measurement can be obtained with the assumption that there is no variation ($n=0$) and a constant dust temperature as given in Table 2. But a fit which is almost as good can be obtained with values of n of 1 or 2; in those cases the dust temperature would have to be decreased.

With each assumption concerning the value of n, and with the consequent value of T_D which follows from fitting the observation, a value of the optical depth of the dust in each nebula as a function of frequency may be computed from

$$4\pi d^2 F_\nu = \frac{4\pi R^2}{3} 2\tau_\nu \pi B_\nu(T_D),$$

where F_ν is the measured flux at frequency ν, d is the distance to the nebula, R is its radius. B_ν is the Planck function and τ_ν is as usual

$$\tau_\nu = Q_\nu \pi a^2 n_d 2R,$$

where a is the radius of the dust and n_d its number density. Since a and n_d are fixed in any given nebula, the variation of τ_ν with frequency is a reflection of the variation of Q_ν. The result of this calculation does not give substantially new information however. When $n=0$ is assumed, the consequent value of T_D leads to a value of τ_ν approximately independent of frequency, while the value of T_D found by assuming $n=1$ leads a value of τ_ν which varies approximately as the first power of the frequency. Thus the results are completely consistent with the assumptions in these two cases. For the case $n=2$ there is generally less consistency.

There is one further piece of information which could shed some light on this question. For those nebulae where the infrared excess (IRE) is greater than 1.5 to 2, the dust must be absorbing energy directly from the star. This means the dust must have a substantial optical depth in the ultraviolet, where most of the stellar energy is found. Thus $\tau_{vis} \sim 0.1$ in these nebulae. Thus an approximate ratio of Q_{IR}/Q_{vis} may be found for each of the assumptions concerning n, and may be compared to other information concerning this ratio.

For the interstellar medium consisting of a mixture dominated by silicate material, the value $Q_{25\,\mu m}/Q_{vis}$ is about $6\,10^{-2}$ (Mathis et al., 1983). This value is consistent with the values of $\tau_{25\,\mu m}$ found with the assumption $n=1$ and $n=2$. It is not consistent with $n=0$. On the other hand, if the material were dominated by graphite, for which $Q_{25\,\mu m}/Q_{vis}$ is about $3\,10^{-3}$ (Mathis et al., 1983) the $n=0$ results would be consistent with the observed τ_{vis}, while the $n=1$ and 2 results would predict too high values of τ_{vis}. It seems likely that the dust in planetary nebulae has less silicate material than the interstellar medium because low resolution spectra in the 8 to 13 μm region show no indication of the 9.7 μm feature usually associated with silicate material. This feature is not seen either in absorption or emission in any of the nebulae studied.

A definite conclusion cannot be made at this time. If the material is similar to that in the interstellar medium, then n is between 1 and 2. If the dust has properties similar to graphite, $n \simeq 0$.

VIII. Dust mass in nebulae

The mass of dust, M_D may be computed from (e.g., Hildebrand, 1983; Barlow, 1983).

$$M_D = \frac{4}{3}\frac{a\varrho}{Q_\nu}\frac{d^2 F_\nu}{B_\nu(T_D)}\,\mathrm{g},$$

where ϱ is the specific density of the dust material in g cm^{-3}. The ratio of dust to gas mass may be written

$$\frac{M_D}{M_g} = \frac{d^2}{R^3}\frac{F_\nu}{\pi B_\nu(T_D)}\frac{a\varrho}{Q_\nu}\frac{4.5\,10^{23}}{n_e}.$$

It may be seen from the above equations that, even if a constant temperature nebula is assumed, the dust mass depends on knowledge of T_D (or n) and the value of a, ϱ, and Q_ν, or at least their ratio's. We will assume for the remainder of this discussion that $\varrho = 3$ g cm^{-3} and $a = 10^{-5}$ cm (Hildebrand, 1983). The dust particle average size is uncertain by as much as an order of magnitude; if other values are preferred for these quantities the dust masses may be appropriately changed. This is the largest uncertainty in the determination of the dust mass. Surprisingly, the uncertainty in the knowledge of T_D plays a much smaller role. This is because the consistent value of Q_ν associated with each of the assumptions $n=0$, 1 and 2 varies in such a way as to cancel the effect of the change in dust temperature. Thus for the temperatures associated with $n=0$, a value of $Q_{25\,\mu m} = 3\,10^{-3}$ is used. This gives the same mass as the temperatures associated with $n=1$ and $Q_{25\,\mu m} = 1.5\,10^{-2}$, or $n=2$ and $Q_{25\,\mu m} = 7\,10^{-2}$. These dust to gas mass ratios are given in the last column of Table 2 using values of n_e given by Pottasch (1984). The dust to gas ratios are also shown in Fig. 6 plotted against the nebular radius. It can be seen that the high values of gas to dust are found in the small, young nebulae, while the ratio decreases by two orders of magnitude in old objects. This qualitatively confirms a similar result found by Natta and

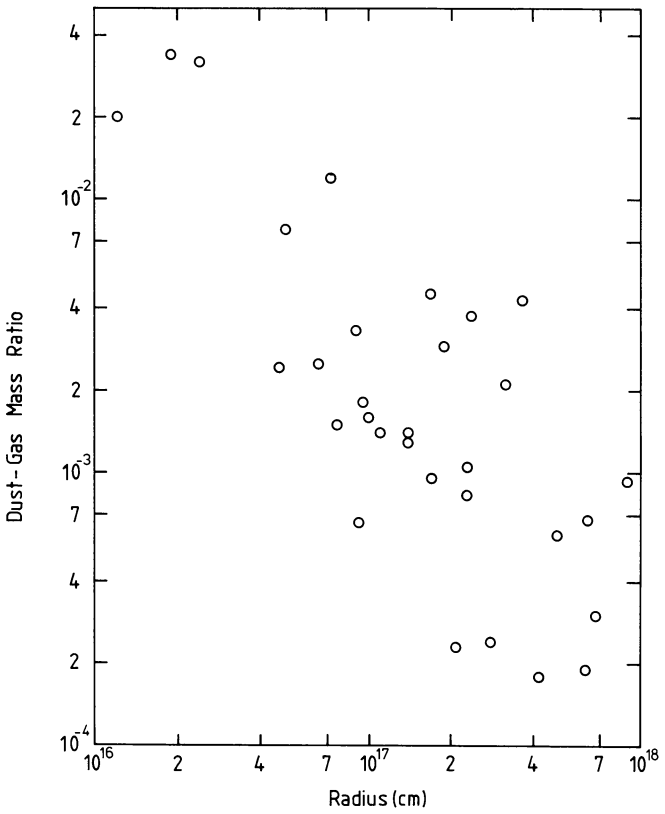

Fig. 6. The ratio of dust mass to gas mass is plotted against the radius of the nebula

Panagia (1981), although the quantitative results are different. While the choice of the dust parameters and especially the average dust radius, is very uncertain, it seems unlikely that the general correlation will prove to be wrong. This would only be the case if the parameters varied in some systmatic way with nebular radius. For example, a constant dust to mass ratio could be obtained by postulating that the average dust size increases strongly with nebular radius. But such a behavior is probably more difficult to explain than the decrease in dust to gas mass.

The variation of dust to gas ratio is largely due to the variation of the ionized gas mass, which is assumed to account for the entire nebular mass. Thus it is implicitly assumed that the dust emission originates in the ionized region. The derived dust mass of the nebulae is listed in the next to last column of Table 2, and has an average value of about $10^{-4} M_{\odot}$, with a large scatter about this value. But the dust mass varies only slightly with nebular radius. One may then ask whether the dust radiation comes from the entire nebula, i.e., both the neutral and ionized parts which would explain the apparent constancy of the dust mass and the change in the dust to gas ratio. There is an important argument against this. Both the dust mass and the dust to gas ratio have been computed assuming the dust is confined with the radius of the ionized nebula. If the neutral material were an important emitter, a larger radius would therefore have to be used for the smaller nebulae which contain the lowest ionized gas masses. This would increase the dust masses of the smallest nebulae more than the large nebulae, which would compensate for the increase in gas mass by including neutral material.

The conclusion appears justified that the material intially emitted in a nebula has a dust to gas mass ratio close to that of the interstellar medium but that in the course of nebular evolution this ratio decreases substantially. It also appears that this initial ratio varies by more than a factor of 10 from nebula to nebula. High values of dust are found especially in NGC 7027 (not observed by IRAS) and NGC 2346.

References

Aitken, D.K., Roche, P.F.: 1983, *Monthly Notices Roy. Astron. Soc.* **202**, 1233

Barlow, M.J.: 1983, *IAU Symp.* **103**, Reidel, Dordrecht, p. 105

Bentley, A.F.: 1982, *Astron. J.* **87**, 1810

Cohen, M., Barlow, M.J.: 1974, *Astrophys. J.* **193**, 401

Cohen, M., Barlow, M.J.: 1980, *Astrophys. J.* **238**, 585

Gillett, F.C., Knacke, R.F., Stein, W.A.: 1971, *Astrophys. J.* **163**, L57

Gillett, F.C., Low, F.J., Stein, W.A.: 1967, *Astrophys. J.* **149**, L97

Gillett, F.C., Stein, W.A.: 1970, *Astrophys. J.* **159**, 817

Higgs, L.A.: 1973, *Monthly Notices Roy. Astron. Soc.* **161**, 313

Hildebrand, R.H.: 1983, *Quart. J. Roy. Astron. Soc.* **24**, 267

Krishna Swamy, K.S., O'Dell, C.R.: 1968, *Astrophys. J.* **151**, L61

Mathis, J.S., Mezger, P.G., Panagia, N.: 1983, *Astron. Astrophys.* **128**, 212

Milne, D.K., Aller, L.H.: 1975, *Astron. Astrophys.* **38**, 183

Milne, D.K., Aller, L.H.: 1983, *Astron. Astrophys. Suppl.* **50**, 209

Moseley, H.: 1980, *Astrophys. J.* **238**, 892

Natta, A., Panagia, N.: 1981, *Astrophys. J.* **248**, 189

Pottasch, S.R.: 1983, *IAU Symp.* **103**, Reidel, Dordrecht, p. 391

Pottasch, S.R.: 1984, Planetary Nebulae, Reidel, Dordrecht

Pottasch, S.R., Beintema, D.A., Raimond, E., v. Duinen, R.J., Habing, H.J., Houck, J., Jennings, R., de Jong, T., Olnon, F., Wesselius, P.R., Baud, B.: 1984, *Astrophys. J. Letters* **278**, L33

Preite-Martinez, A., Pottasch, S.R.: 1983, *Astron. Astrophys.* **126**, 31

Shure, M.A., Herter, T., Houck, J.R., Briotta, D.A., Jr., Forrest, W.J., Gull, G.E., McCarthy, J.F.: 1983, *Astrophys. J.* **270**, 645